Uniport Journal of Engineering and Scientific Research (UJESR)

Vol. 5, Special Issue, 2020, Page 81-94
ISSN: 2616-1192

(www.ujesr.org)

Modeling and Investigating the Effect of Offset Distance on Slider-Crank Mechanism

Obaseki, M*[1] and Alfred, P.B[2]
[1]Department of Mechanical Engineering, Faculty of Engineering, Nigeria Maritime University, Okerenkoko, Nigeria
[2]Department of Mechanical Engineering, Faculty of Engineering, University of Port Harcourt, Port Harcourt, Nigeria
*Corresponding author's email: martins.obaseki@nmu.edu.ng

Abstract
Slider-crank mechanism is a mechanical system which forms a part of larger mechanical systems such as internal combustion engines, reciprocating pumps, pneumatic devices and feeders. Modeling of slider-crank mechanism is aimed at predicting crank and slider positions at any given time with respect to the fixed positions known as the dead centers. In this work, emphasis is on effect of offset distance on the performance of an offset slider-crank mechanism, using both geometry and trigonometry. Dynamic and kinematic models were developed with the offset distance term factored in such that it can be varied and its effect on the position, velocity, acceleration, forces and torque observed. The models were used to analyze the effect of offset distance on the acceleration and torque. Findings show that; offset slider-crank mechanism has maximum acceleration and torque in one stroke, and that the maximum torque increases with increase in offset distance. The models can predict with high degree of accuracy the position of maximum acceleration, minimum and maximum torque. The models in this work can be used in the design and fabrication of slider-crank mechanism in mechanical systems that required high acceleration and torque in one stroke.

Keywords: *Slider-crank model, Offset slider-crank mechanism, Geometry, Instantaneous velocity, Instantaneous acceleration*

Received: 22nd May, 2020 *Accepted: 21st June, 2020*

1. Introduction

Slider-crank mechanism is a mechanical system in which rotary motion is converted to reciprocating motion and vice versa using three components namely, the crank, the slider and the connecting rod. The crank centre and the slider block centre may be in line or offseted (Sahidur, 1991; Julius, 2016). The slider-crank mechanism finds its application in reciprocating pump, internal combustion (IC) engines, pneumatic valves etc. In the reciprocating pump, the piston sucks in the product to be pumped by sunction pressure, and then, the return stroke pushes out the product to be pumped out in the forward stroke. The sunction stroke required lesser torque than the pumping stroke. The input force for the slider-crank mechanism in reciprocating pump comes from the motor shaft which supplies the rotational force to the crank that is transferred to the piston through the connecting rod. In Internal Combustion (IC) Engine, the input force to the slider-crank mechanism comes from the combustion of gas in the engine cylinder. The combusting gas expands thereby exerting pressure on the piston which then transfers the force to the crank, and causes rotation the engine shaft.

In industries, the slider-crankmechanisms are used in automated feeders. Automated feeders are machine structures which pushes and compacts materials to be processed into the processing chambers (Sarigeçili and Akçali, 2018). The forward stroke requires a greater torque to compact and press the materials into the machine while the return stroke requires less torque. To achieve this, slider-crank mechanism has to be modified to produce more torque in the forward stroke. The offset slider-crank mechanism is useful for producing more torque, and proper modeling will reveal the likely position of the crank and the slider where maximum torque values are produced.

Slider-crank mechanism can also be used in the construction of robotic limbs. Doyoung et al. (2013) designed a slider-crank leg for mobile hopping robotic platforms. In their work, an attempt was made to design a new leg for a mobile robot using the slider-crank mechanism to change

the rotary motion of the electric motor into a linear motion of the slider (piston) with which the mobile robot impacts the ground. Slider-crank mechanism that will function best in this machine will have to produce more torque in one stroke over the other because it will require more torque to hop than the other processes of the mobile hopping robot. Devices here require torque difference between the forward stroke and the reverse stroke, thus, the need to develop a model that will account for torque difference in offset slider-crank mechanism.

So much research work has been carried out on slider-crank mechanism, most of which are directed to modeling and prediction of kinematic performance of the mechanism. Shrikant et al. (2013) carried out a review on a slider-crank mechanism with the aim of understanding the kinematic and dynamic performance of the different mechanisms and possibly modifying them. Sarigeçili et al. (2018) used the lumped mass approach to model a slider-crank mechanism which can accept varying input parameters for any required piston speed. Mohammad et al. (2011) carried out a research on the kinematic and kinetic analysis of slider-crank mechanism using a linear Otto IC engine with four cylinders. The works of Julius (2016), Rudolf et al. (2012) and Boyle et al. (1997) are all on offset slider-crank mechanism with the aim of optimizing its kinematic performance. Though it has been established that torques depend on kinematic quantities, the issue of crank or slider position at which maximum and minimum torques can be obtained is yet to be addressed. Also, the investigation of the effect of offset distance on acceleration and torque developed in the slider-crank mechanism is lacking in literature. Therefore, it is appropriate to say that the issue of torque difference of the forward and the reverse stroke and their applications have not been clearly addressed. Thus, the objective of this work is to model an offset slider-crank mechanism in such a way that the effect of offset distances and position of maximum torque can be properly investigated. The model developed in this work can be seen as a modification of existing model in which offset distance term has been incorprated. The offset distance term, which can be plotted and examined at varying conditions of the system and the performance of the system observed. The model forms the basis for the design processes of the offset slider-crank mechanism at any offset distance. It can used to analyse the the effect of offset distance on maximum torque produced in the forward and backward stroke of the mechanism.

2. Kinematic modeling of slider-crank mechanism

The slider-crank mechanism is shown in Fig. 1. The crank rotates in a circular part thereby transmitting reciprocating motion onto the slider block through the connecting rod (Mohammad et al., 2011). The slider block moves between two centers C_1 and C_2 which corespond to Botom Dead Centre (BDC) and Top Dead Centre (TDC) of IC engine cylinnder (Rudolf et al., 2012). The distance from C_1 to C_2 is known as the stroke (Rudolf et al., 2012).

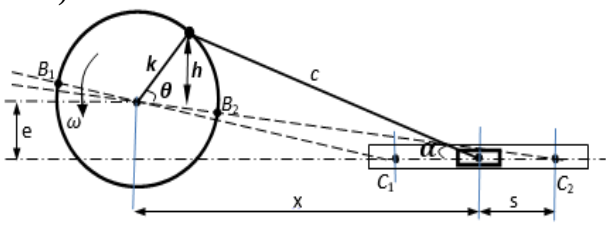

Fig 1: Offset slider-crank mechanism

The slider-crank mechanism can be driven from either the crank end as in reciprocating pump (Santosh et al., 2018) or the slider block end as in automotive engiine (Santosh et al., 2018; Sarigeçili et al., 2018). In both cases, the kinematics of the slider block can be modeled to be a function of the crank angle and the lengths of the crank and connecting rod using either analytical or graphical method (Patel et al., 2013). In this work analytical modeling was employed to model the mechanism starting from the crank end. The modeling in this study take into consideration the offset distance (e) which make it impossible to use simplified trigonometrical identities, thus we have a more complex trigonometry in our model and such model has not been recorded in literature. This model can be seen as "modification of existing model" which involve non-easy steps of handling complex trigonometry to add an offset distance term into the existing model. The instantaneous position, velocity and acceleration equations of crank, connecting rod and the slider all have offset distance (e) which make it easy to study the effect of offset distances on the performance of the mechanism.

2.1 The crank

The crank instataneous position is described by the angular displacement θ also known as the crank angle. The crank angle (θ) represents the crank instantaneous position and is defined in radian (Hroncová et al., 2016) in Equation (1):

$$\theta = \omega t \quad (1)$$

where ω is the angular velocity and t is the time. The crank instantaneous angular velocity is the first

derivative of crank displacement equation and it is given in Equation (2).

$$\frac{d\theta}{dt} = \omega \quad (2a)$$

The equivalent liner velocity, v_k, due to changing direction is given as (Peter et al., 2015):

$$v_k = \omega \frac{d\theta}{dt} = \omega k \quad (2b)$$

where k is the crank length. Since the crank rotates at constant angular velocity, the angular acceleration is zero, but the centripetal acceleration (a_k) is given as:

$$a_k = \omega^2 k \quad (3)$$

2.2 Slider block instantaneous position (s)

The distance, x, between the crank Centre and the slider Centre can be determined in terms of crank angle (Jomartov et al., 2015; Santosh et al., 2018; Gregory et al., 2011). From the geometry of Fig.1, x is given as:

$$x = k\cos\theta + c\cos\alpha \quad (4)$$

where α is the angle between the connecting rod and the sliding axis. Also, from Fig.1:

$$h = k\sin\theta \quad (5a)$$

$$h + e = c\sin\alpha \quad (5b)$$

where h is the crank end vertical distance from the centre, e is the offset distance and c is the length of the connecting rod. Combining Equations (5a) and (5b) gives:

$$\sin\alpha = \frac{e}{c} + \frac{k}{c}\sin\theta \quad (6)$$

Using trigonometrical identity, Equation (7) was obtained.

$$\cos\alpha = \frac{1}{c}[c^2 - (e + k\sin\theta)^2]^{1/2} \quad (7)$$

Substituting Equation (7) in Equation (4) gives:

$$x = k\cos\theta + [c^2 - (e + k\sin\theta)^2]^{1/2} \quad (8)$$

The slider block instantaneous position (**s**) is obtained from the slider-crank mechanism geometry as (Kittur et al., 2017):

$$s = k + c - x \quad (9)$$

Substituting Equation (8) into Equation (9):

$$s = (k + c) - k\cos\theta + [c^2 - (e + k\sin\theta)^2]^{\frac{1}{2}} \quad (10)$$

2.3 Slider block instantaneous velocity (v_s)

The instantaneous velocity of the slider block can be determined by differentiating the stroke equation with respect to time (Bhupesh et al., 2013; Boyle et al., 1997).

$$v_s = \frac{ds}{dt} = \frac{ds}{d\theta}.\frac{d\theta}{dt} \quad (11)$$

Differentiating Equation (9) gives:

$$\frac{ds}{d\theta} = k\sin\theta + \frac{k\cos\theta\,(e + k\sin\theta)}{[c^2 - (e + k\sin\theta)^2]^{1/2}} \quad (12)$$

The instantaneous velocity of the slider block is given by Equation (13).

$$v_s = \omega k\sin\theta + \frac{\omega k\cos\theta\,(e + k\sin\theta)}{[c^2 - (e + k\sin\theta)^2]^{1/2}} \quad (13)$$

2.4 Slider block instantaneous acceleration (a_s)

The slider block instantaneous acceleration is determined by taking the first derivative of the instantaneous velocity (Bhupesh et al., 2013; Doyoung et al., 2013; Boyle et al., 1997).

$$a_s = \frac{dv_s}{dt} = \frac{dv_s}{d\theta}.\frac{d\theta}{dt} \quad (14)$$

Let

$$v_1 = \omega k\sin\theta\,; v_2 = \frac{\omega k\cos\theta\,(e + k\sin\theta)}{[c^2 - (e + k\sin\theta)^2]^{\frac{1}{2}}} \quad (15)$$

Then v_s and $\frac{dv_s}{d\theta}$ are redefined as:

$$v_s = v_1 + v_2 \text{ and } \frac{dv_s}{d\theta} = \frac{dv_1}{d\theta} + \frac{dv_2}{d\theta} \quad (16)$$

Taking the derivative of Equation (15) gives Equations (17) and (18).

$$\frac{dv_1}{d\theta} = -\omega k\cos\theta \quad (17)$$

$$\frac{dv_2}{d\theta} = -\frac{\omega k(kcos2\theta - e\sin\theta)}{[c^2 - (e + k\sin\theta)^2]^{\frac{1}{2}}} - \frac{\omega k^2\cos^2\theta\,(e + k\sin\theta)^2}{[c^2 - (e + k\sin\theta)^2]^{\frac{3}{2}}} \quad (18)$$

The equation for the instantaneous acceleration is determined by Equation (19) as:

$$a_s = \frac{dv_s}{dt} = \omega\frac{dv_1}{d\theta} + \omega\frac{dv_2}{d\theta} \quad (19)$$

Substituting Equations (17) and (18) into Equation (19) gives the formula for instantaneous acceleration in Equation (20).

$$a_s = -\omega^2 k\cos\theta - \frac{\omega^2 k(kcos2\theta - e\sin\theta)}{[c^2 - (e + k\sin\theta)^2]^{1/2}} - \frac{[\omega k\cos\theta\,(e + k\sin\theta)]^2}{[c^2 - (e + k\sin\theta)^2]^{3/2}} \quad (20)$$

2.5 Connecting rod instantaneous position (α)

The motion of the connecting rod is a to and fro motion described by the value of α. Equation (4) defined α as:

$$\sin\alpha = \frac{e}{c} + \frac{k}{c}\sin\theta$$

Let

$$\gamma = \frac{e}{c} \text{ and } \delta = \frac{k}{c} \quad (21)$$

Putting Equation (21) into Equation (4) gives Equation (22).

$$\alpha = \sin^{-1}(\gamma + \delta\sin\theta) \quad (22)$$

2.6 Connecting rod instantaneous velocity (v_c)

Differentiating Equation (22) with respect to time gives the equation of instantaneous velocity of the connecting rod.

$$v_c = \frac{d\alpha}{dt} = \frac{d\alpha}{d\theta}.\frac{d\theta}{dt} \quad (23)$$

By implicit differentiation $\frac{d\alpha}{d\theta}$ is determined as follows:

$$\cos\alpha \frac{d\alpha}{d\theta} = \delta\cos\theta \quad (24)$$

$$\frac{d\alpha}{d\theta} = \frac{\delta\cos\theta}{\cos\alpha} \quad (25)$$

The instantaneous velocity is given in Equation (26).

$$v_c = \frac{\omega\delta\cos\theta}{\cos\alpha} \quad (26)$$

Substituting Equation (5b) into Equation (26) and simplifying gives the expression for the connecting rod instantaneous velocity in Equation (27).

$$v_c = \frac{\omega k\cos\theta}{\sqrt{c^2-(e+k\sin\theta)^2}} \quad (27)$$

2.7 Connecting rod instantaneous acceleration (a_c)

The instantaneous acceleration of the connecting rod is determined by Equation (28).

$$a_c = \frac{dv_c}{dt} = \frac{dv_c}{d\theta}.\frac{d\theta}{dt} \quad (28)$$

The differentiation of the velocity equation with respect to theta of the connecting rod in Equation (27) by quotient rule gives Equation (29).

$$\frac{dv_c}{d\theta} = \frac{-\omega k\sin\theta}{[c^2-(e+k\sin\theta)^2]^{1/2}} - \frac{\omega k^2\cos^2\theta\,(e+k\sin\theta)}{[c^2-(e+k\sin\theta)^2]^{3/2}} \quad (29)$$

Substituting ω for $\frac{d\theta}{dt}$ in Equation (28), the equation for connecting rod instantaneous acceleration becomes:

$$a_c = \frac{-\omega^2 k\sin\theta}{[c^2-(e+k\sin\theta)^2]^{1/2}} - \frac{\omega^2 k^2\cos^2\theta\,(e+k\sin\theta)}{[c^2-(e+k\sin\theta)^2]^{3/2}} \quad (30)$$

3. Materials and methods

3.1 Modeling of dynamic forces and torque on slider-crank mechanism

The entire mechanism experiences dynamic forces at different points due to acceleration of masses. The masses which include the crank, the connecting rod and the slider block undergo rotating and reciprocating motion; accelerating and retarding in the process, thus, experiencing dynamic and none uniform forces. Here, mathematical approach is employed to model the dynamic load in the slider-crank mechanism. Force on a body has been defined by Isaac Newton as the product of mass and the acceleration of the body. Torque on the other hand is the product of force and the perpendicular distance from the point of action of the force. Thus, force and torque are functions of mass and acceleration. Acceleration equations of crank (a_k), connecting rod (a_c) and the slider (a_s) have been modeled in Section 2 to include the offset distance (e). The dynamic forces and torques on the slider-cranker mechanism depend on these accelerations. Therefore, including the accelerations (a_k, a_c *and* a_s) result in the modified models recorded in this section.

3.2 Equivalent rotating and reciprocating masses

Modeling dynamic forces in the system requires the accurate modeling of the actual masses constituting the inertia forces on the system (Hailemariam, 2015; Bhupesh et al., 2013). These masses which are the equivalent circulating mass and reciprocating mass must be accurately modeled. The rotating mass is the equivalent mass at point 2 in Fig. 2 and the reciprocating mass is the equivalent mass at point 3.

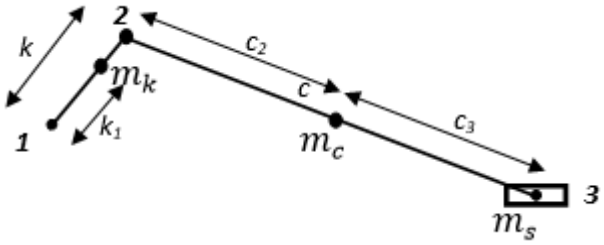

Fig. 2: Mass balance of offset slider-crank mechanism

Let $m_c = mass\ of\ connecting\ rod$, $m_k = mass\ of\ crank$ and $m_s = mass\ of\ slider\ block$. The mass of the connecting rod is sum of its equivalent mass at the reciprocating end (m_{3c}) and that at the rotating end (m_{2c}).

$$m_c = m_{2c} + m_{3c} \quad (31)$$

Taking moment about point 3 gives the equivalent mass of connecting rod at the Rotating end and at reciprocating end as:

$$m_{2c} = m_c\frac{c_3}{c} \quad (32)$$

$$m_{3c} = m_c\frac{c_2}{c} \quad (33)$$

The total reciprocating mass (equivalent mass at point 3) is the sum of equivalent mass of

connecting rod at the reciprocating end and the mass of the slider.

$$m_3 = m_{3c} + m_s \quad (34)$$

The equivalent mass of crank at the rotating end is determined by taking moment about point 1.

$$m_{2k} = m_k \frac{k_1}{k} \quad (35)$$

The total rotating mass (equivalent mass at point 2) is the sum of equivalent mass of connecting rod at the rotating end and the equivalent mass of the crank at the rotating end.

$$m_2 = m_{2c} + m_{2k} \quad (36)$$

3.3 Modeling of dynamic forces and torque

The diagram in Fig. 3 shows the forces acting on the system. The model assumed that a constant external force on the crank caused it to rotate uniformly at an angular velocity of ω rad/s in the anticlockwise direction.

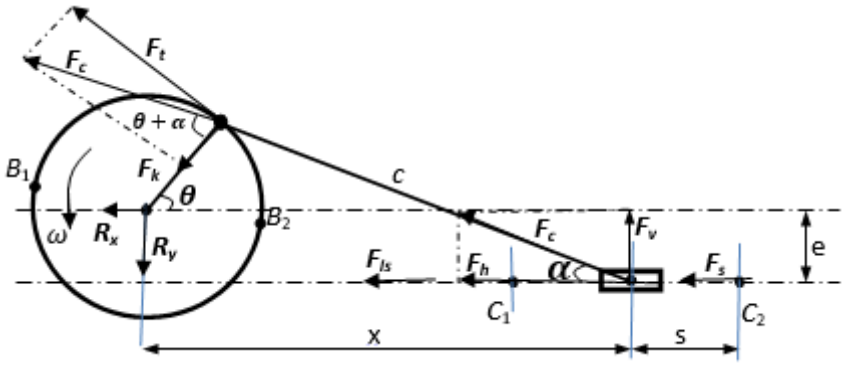

Fig. 3: Force analysis of offset slider-crank mechanism

3.3.1 Forces on the system

a. Inertial force on the crank (F_k)

The inertial force on the crank is the force on the crank due to its acceleration. The acceleration of the crank is directed towards the crank centre; thus, the direction of the inertia force is towards the centre as shown in Fig. 3. The inertia force on the crank is calculated by multiplying the equivalent rotating mass by the acceleration of the crank (Hailemariam, 2015; Eric et al., 2013).

$$F_k = m_2 a_k = m_2 \omega^2 k \quad (37a)$$

Equation (37a) resolved into component form gives:

$$F_k = -(m_2 \omega^2 k \cos\omega t)\hat{\boldsymbol{\imath}} - (m_2 \omega^2 k \sin\omega t)\hat{\boldsymbol{\jmath}} \quad (37b)$$

b. Reactions at the crank centre (R_x and R_y)

From Equation (37b) the reactions at the crank pin are:

$$R_x = -m_2 \omega^2 k \cos\omega t \quad (38)$$

$$R_y = -m_2 \omega^2 k \sin\omega t \quad (39)$$

c. Tangential force on the crank (F_t)

This is the force acting tangential to the circle part of the motion of the crank head. The direction of the tangential force coincides with the direction of the velocity at any point on the part of crank motion. The tangential force is determined from the geometry of the forces in Fig. 3.

$$F_t = F_k \tan(\alpha + \theta) \quad (40)$$

d. Force on the connecting rod (F_c)

This is the axial force transmitted along the connecting rod to the slider block. The axial force on the connecting rod is determined by resolving the inertial force based on the geometry in Fig. 3.

$$F_c = \frac{F_k}{\cos(\alpha + \theta)} \quad (41)$$

e. Inertial force on the slider block (F_{Is})

The inertia force on the slider block is the force on the block due to its acceleration. The motion of the slider is reciprocating, thus the acceleration changes at every interval. The inertia force on the slider block is calculated by multiplying the equivalent reciprocating mass by the acceleration of the slider block (Hailemariam, 2015; Sahidur et al., 1991; Mohammad et al., 2011).

$$F_{Is} = -m_3 a_s \ \hat{\imath} \quad (42a)$$

$$F_{Is} = m_3 \left[\omega^2 k \cos\theta + \frac{\omega^2 k (k - 2k\sin^2\theta - \sin\theta)}{[c^2 - (e + k\sin\theta)^2]^{1/2}} - \frac{[\omega k \cos\theta\,(e + k\sin\theta)]^2}{[c^2 - (e + k\sin\theta)^2]^{3/2}} \right] \quad (42b)$$

f. Horizontal force on the slider transmitted by the connecting rod (F_h)

The horizontal force on the slider is the horizontal component of the axial force transmitted by the connecting rod. It is calculated using Equation (43).

$$F_h = F_c \cos\alpha \quad (43)$$

g. Vertical force on the slider transmitted by the connecting rod (F_v)

The vertical force on the slider is the vertical component of the axial force transmitted by the connecting rod. It is calculated as:

$$F_v = F_c sin\alpha \quad (44)$$

h. Total force on slider block

The total force on the slider is the sum of inertia force on the slider and the horizontal component of the axial force on the connecting rod transmitted to the slider block.

$$F_s = F_{Is} + F_c cos\alpha \quad (45)$$

i. Total inertia force on the system

This is the sum of the inertia force on the rotating crank and that of the reciprocating slider block. It is determined as:

$$F_I = -(m_2\omega^2 k\, cos\omega t + m_3 a_s)\hat{\boldsymbol{\imath}} - (m_2\omega^2 k\, sin\omega t)\hat{\boldsymbol{\jmath}} \quad (46a)$$

The slider is constrained to move in x – direction, thus the horizontal component of the inertial force is given in Equation (46b).

$$F_i = -(m_2\omega^2 k\, cos\omega t + m_3 a_s)\hat{\boldsymbol{\imath}} \quad (46b)$$

3.3.2 Torque on the system

a. Torque on the crank

The torque on the crank is the product of the inertia force on crank and the crank length.

$$T_k = R_x k = -k m_2\omega^2 k\, cos\omega t \quad (47)$$

b. Total torque on the system

The torque on the Slider-crank mechanism is the product of the inertia force perpendicular to the crank and the crank length (Hailemariam, 2015).

$$T = kF_i tan\alpha \quad (48)$$

4. Results and discussion

To generate results, MATLAB scripts was developed based on Equations (1-48). The scripts were used to generate results and analyze the results generated. The flow chart for development of the script is given in Fig. 4.

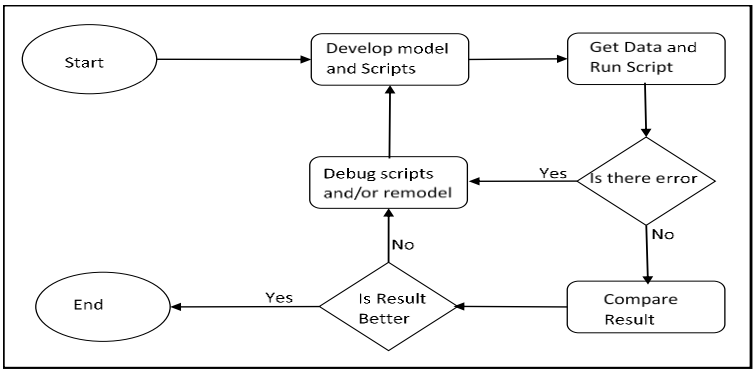

Fig. 4: Flow chart for development of Matlab script

4.1 Input data

The input data used for running the scripts are given in Table 1. The data were chosen based on real data obtained from Laboratory prototyped slider-crank mechanism. The crank is assumed to be running at a constant speed of 2400 rev/min (251rad/s) as a result of external force connected to it. The length of the connecting rod and the crank were calculated from the maximum stroke length using the relation in Equations (49) and (50). A maximum stroke length of 80mm was used for the design.

$$s = 2k \quad (49)$$

$$c = 3.2e \quad (50)$$

Table 1: Input data for analysis

Data description	Value	Unit
Angular Velocity [ω]	251	Rad/s
Frequency [N]	2400	Rev/min
Maximum Stroke [S]	80	Mm
Crank Length [k]	40	Mm
Crank Mass [M_k]	0.2	Kg
Length of Connecting Rod [c]	64	Mm
Mass of Connecting Rod [M_c]	0.5	Kg
Offset distance [e]	20	Mm

Mass of Slider $[M_s]$	0.8	Kg
Time range (t)	0.01 – 0.06	S

4.2 Result analysis

4.2.1 Kinematics result

The input data were used to generate results using the MATLAB script developed for the purpose. The results show that the mechanism is a quick return mechanism because it runs with a time constant of approximately 1.08. The time and crank angle of the return stroke are 0.12 seconds and 172.57^0 respectively, while that of the forward (advance) stroke are 0.13 seconds and 186.96^0 respectively. Time constant (Q) is calculated as (Julius, 2016):

$$Q = \frac{\text{Time of advance stroke}}{\text{Time of return stroke}} = \frac{\text{Advance crank angle}}{\text{Return crank angle}} \quad (51)$$

The forward stroke is the stroke when the slider moves to the right and it corresponds to crank angle range of 172.57º - 359.53º, while in the return stroke, the slider moves to the left and it corresponds to crank angle range of 0º - 172.57º. This is so because the crank moves in an anticlockwise direction (Fig. 3). The maximum stroke length of the Slider-crank mechanism is 0.08m (80mm) and the period is 0.025 seconds which corresponds to 360º crank angle. The stroke pattern is shown in Fig. 5 and Fig. 6.

Figures 7 and 8 show that the velocity and acceleration time graphs of the slider block are not sinusoidal but take the shapes shown in the figures. The velocity of the return stroke is higher than that of the forward stroke (Quick return mechanism). Fig. 7 shows a steeper slop at return stroke and a meandered slope at forward stroke. Fig. 8 shows that the acceleration is always in the direction of advancement; thus, acceleration is positive and has a higher value at positive stroke and a negative lower value at return stroke.

Figures 9 and 10 are respectively the velocity-time graph and the acceleration-time graph of the connecting rod. The period of the connecting rod is the same with the crank but its pattern is more like a cosine function, although it has a steeper slope at return stroke than forward stroke.

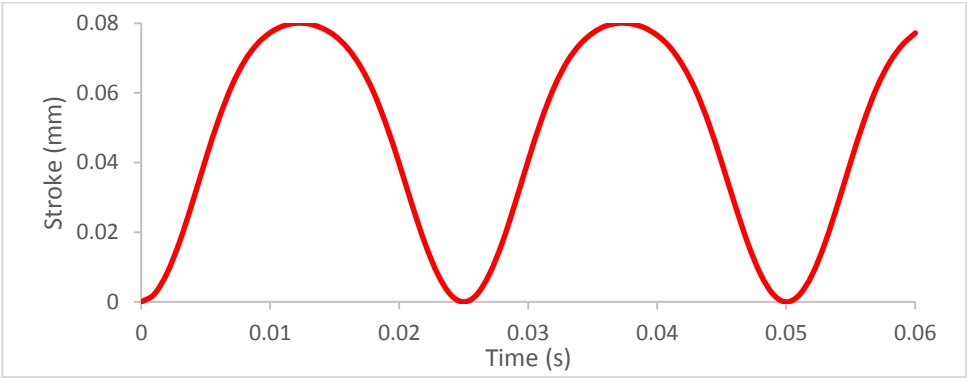

Fig. 5: Stroke-time graph

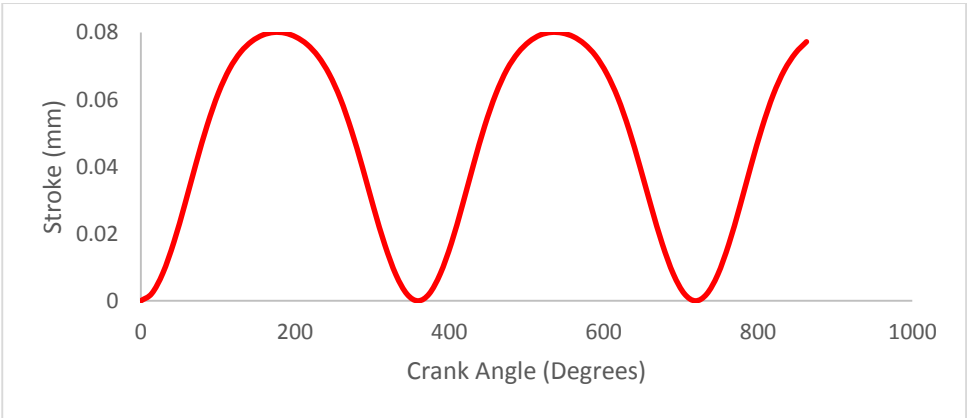

Fig.6: Stroke versus crank angle graph

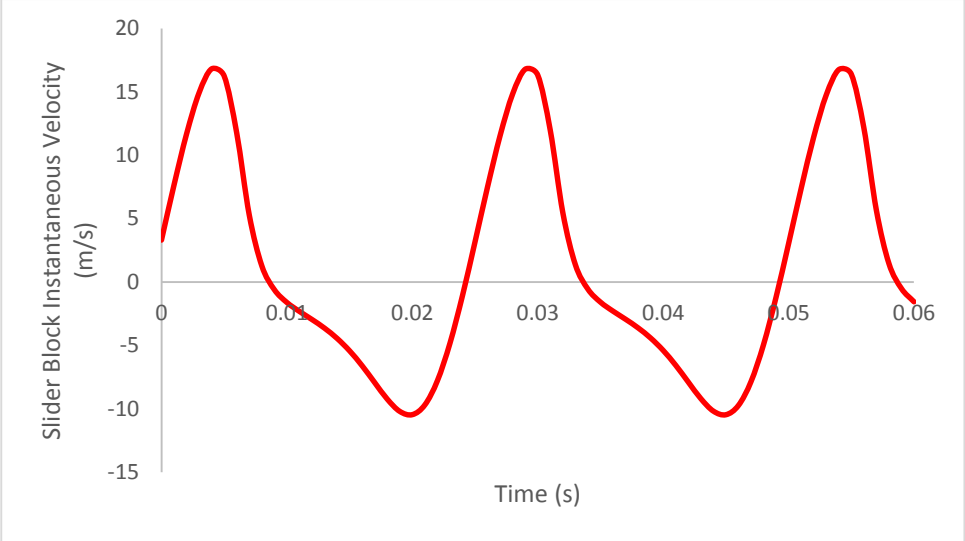

Fig. 7: Velocity-time graph of slider block

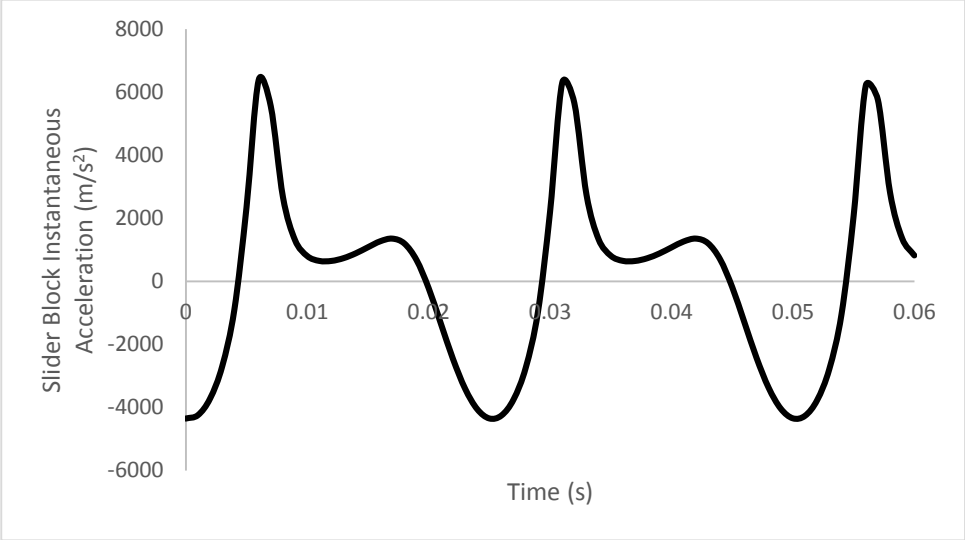

Fig. 8: Acceleration-time graph of slider block

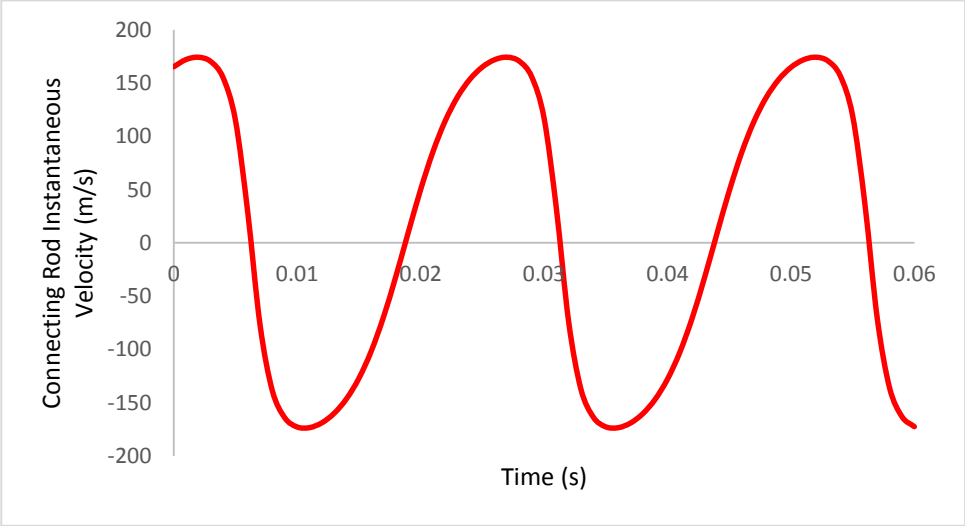

Fig. 9: Velocity-time graph of connecting rod

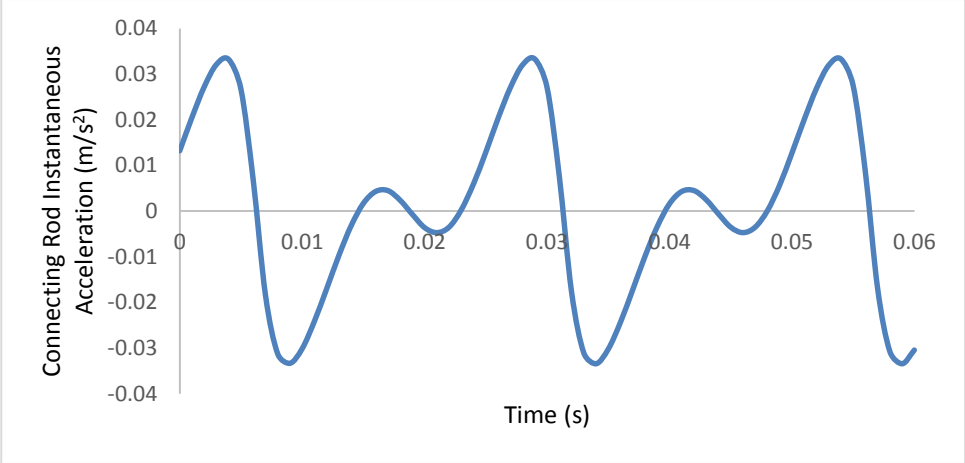

Fig. 10: Acceleration-time graph for connecting rod

4.2.2 Dynamic forces and torque analysis

The forces on the system that are of utmost significance are the reactions at the crank pin and the inertia forces. The reactions are also known as shaking forces because they are transmitted in the surrounding of the mechanism and cause vibration of the ground plane of machine (Eric et al., 2013). The reaction forces are the ones causing shearing stresses in the crank pin and can lead to failure if the pin is not properly designed. Figures 11 and 12 show the horizontal and vertical reaction (shaking) forces on the crank pin.

The inertia forces are the forces caused by the acceleration of the system. Fig. 13 shows the total inertia forces on the system. This is the sum of the horizontal shaking force of the crank and the force cause by acceleration of the slider block. The total inertia force is responsible for producing torque in the mechanism. Fig 14 shows the total torque on the system when the offset distance is 20mm. The results in Figigures 13 and 14 are consistent with those obtained by Mohammad et al. (2011) using MS ADAMS Software. The figure shows that the return stroke has higher torque of about 250Nm developed over a shorter period than the advance stroke which is less than 50Nm developed over a much longer interval compared to that of the return stroke. This is so because the crank rotates in anticlockwise direction. The higher torque produced can be used in advance stroke if the crank direction of rotation is changed to clockwise with the same angular velocity.

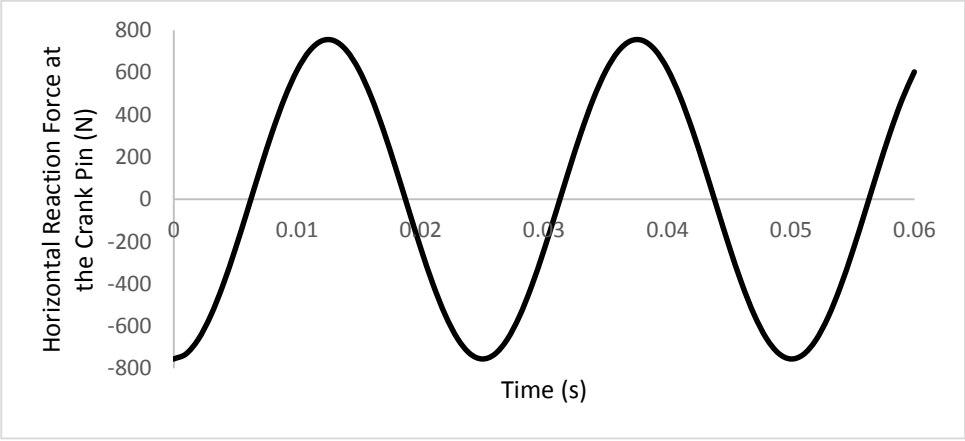

Fig. 11: Horizontal reaction force at the crank pin

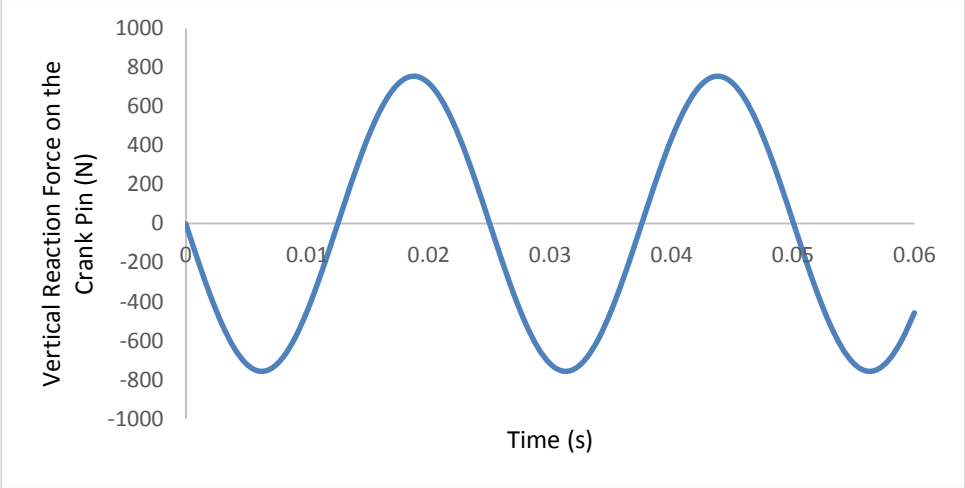

Fig. 12: Horizontal reaction force at the crank pin

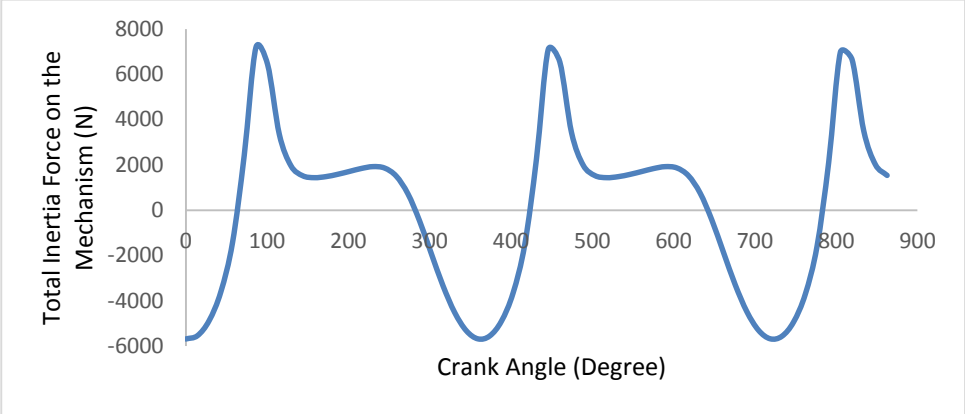

Fig. 13: Total inertia force on the mechanism

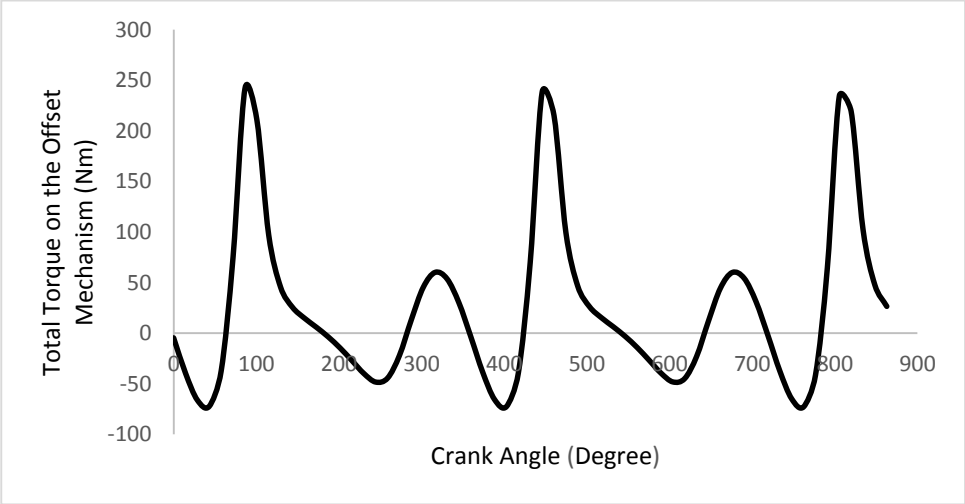

Fig. 14: Total torque on the mechanism

4.3 Torque analysis

Figures 15 and 16 show the results of the comparison of the acceleration and torque developed in the mechanism at different offset distances (e) over two cycles of the crank rotation. At e = 0 (dynamically balanced mechanism), the total torque is about 80Nm and are almost equal in both advance and return stroke. Fig. 16 shows that at e = 10mm, the total torque produced in the system is about 120Nm in the return stroke and 50Nm in the advance stroke, and at e = 20mm, the total torque produce rose to about 250Nm in the return stroke but less than 50Nm in the advance stroke. The figure shows that a much higher torque

in one stroke can be achieved in offset mechanism than in normal mechanism, thus, system requiring higher one directional torque can be analyzed using the present model.

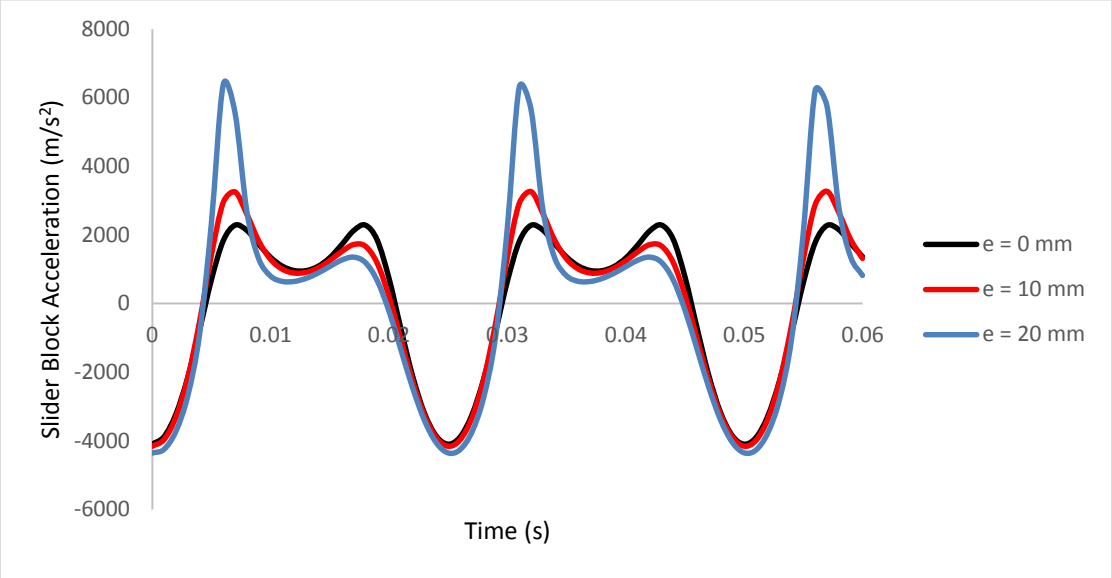

Fig. 15: Effect of offset distance on acceleration of slider

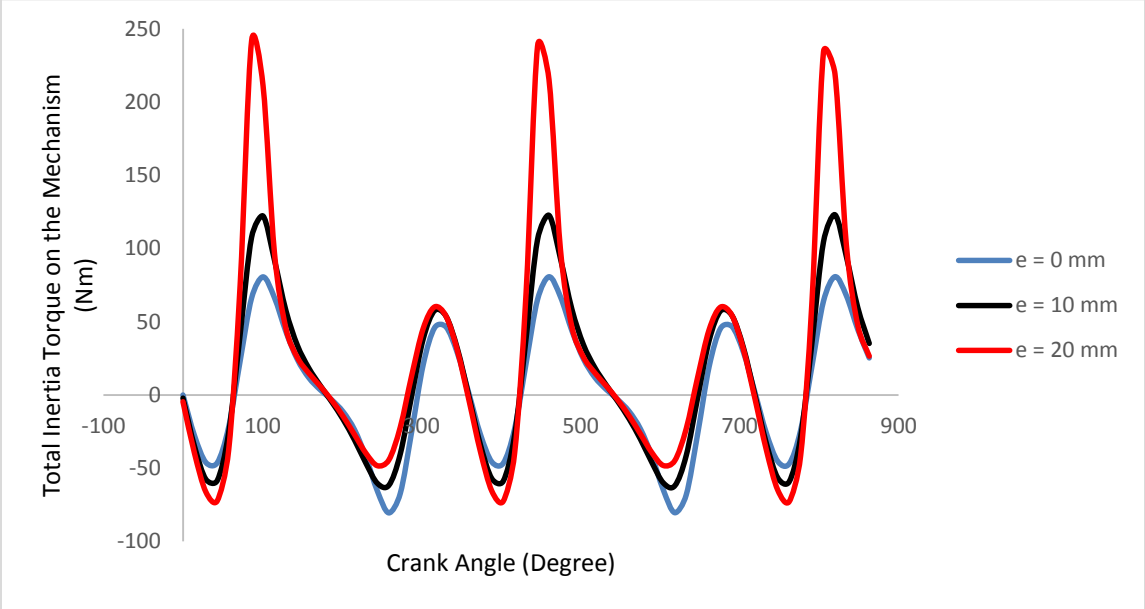

Fig. 16: Effect of offset distance on total torque

4.4 Comparison with existing model

According to Hailemariam (2015), the acceleration and the torque of a Slider-crank mechanism such as that of an automotive engine are modeled by the Equations (52) and (53).

$$a_{is} = -k\omega^2[\,cos\omega t + \delta cos2\omega t] \quad (52)$$

$$T_i = m_3 k^2 \omega^2 \left[\frac{ksin\theta}{4c} - \frac{sin2\theta}{2} - \frac{3ksin3\theta}{4c}\right] \quad (53)$$

Equations (52) and (53) are termed "Existing model" and the model in this work is termed "This model". The existing model and this model where compared and the results are shown in Figures 17 and 18.

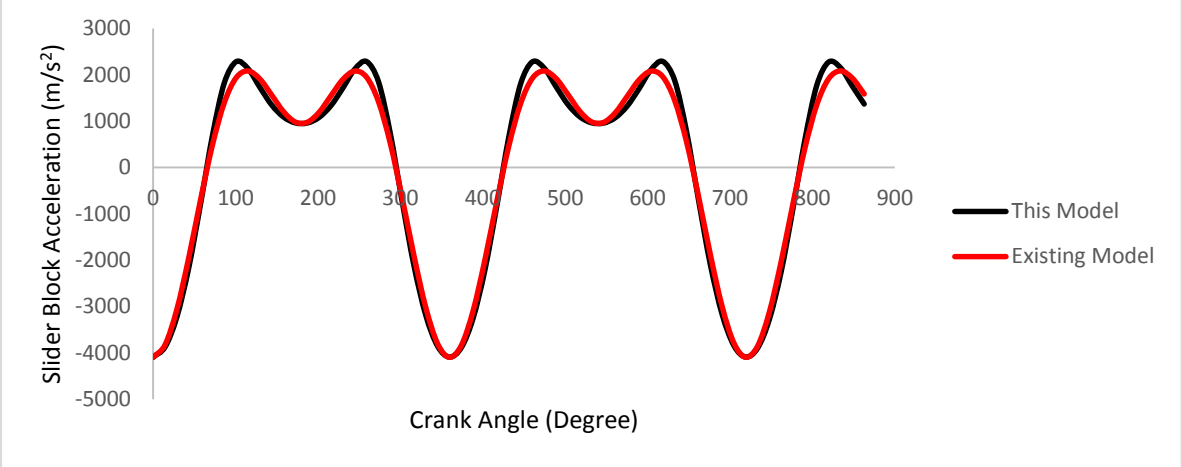

Fig. 17: Comparing acceleration with existing model

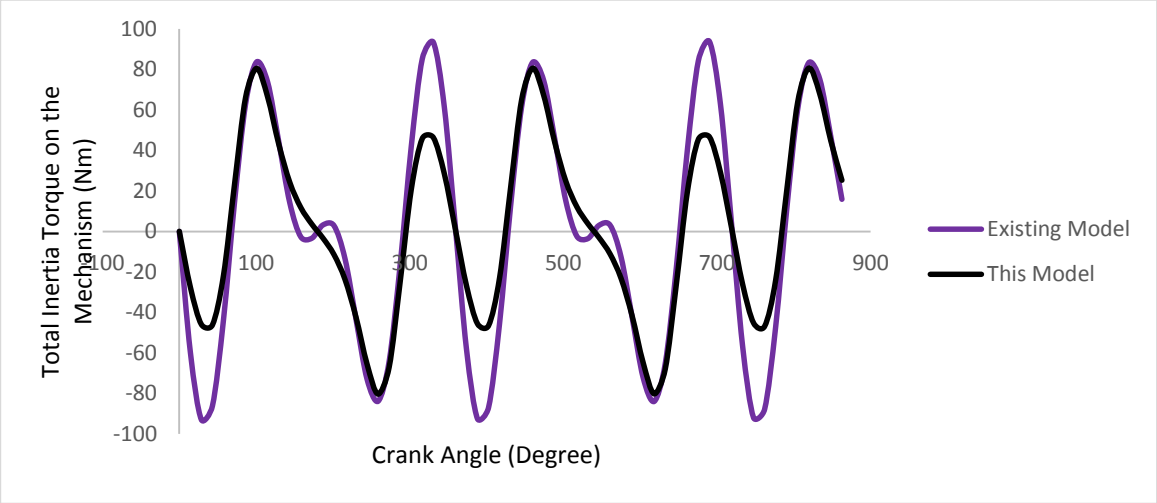

Fig. 18: Comparing torque with existing model at e = 0mm

4.5 Comparison with experimental values

An experimental result of Eric et al. (2013) was extracted and used to test this model. The data in Table 2 were used in the experiment. The Slider-crank mechanism used for the experiment where constructed by Eric et al. (2013) and the machine was run with gas with unsteady pressure. However, the angular speed was measured to be approximately 200rev/min. In other to test the model in this work, the offset distance was set to zero (e = 0) to convert the model to dynamically balanced slider-crank mechanism model. The experiment values were extracted from the acceleration plot of the instruments used by Eric et al. (2013).

Table 2: Input data for experimentation (Eric et al., 2013)

Data description	**Value**	**Unit**
Average Angular Velocity [ω]	20.994	Rad/s
Average Revolution [N]	200	Rev/min
Crank Length [k]	38.1	Mm
Equivalent Rotating Mass [M_2]	7	Kg
Length of Connecting Rod [c]	152.4	Mm
Equivalent Reciprocating Mass [M_3]	1.543	Kg
Offset distance [e]	0	Mm
Time range (t)	0.01 – 0.6	S

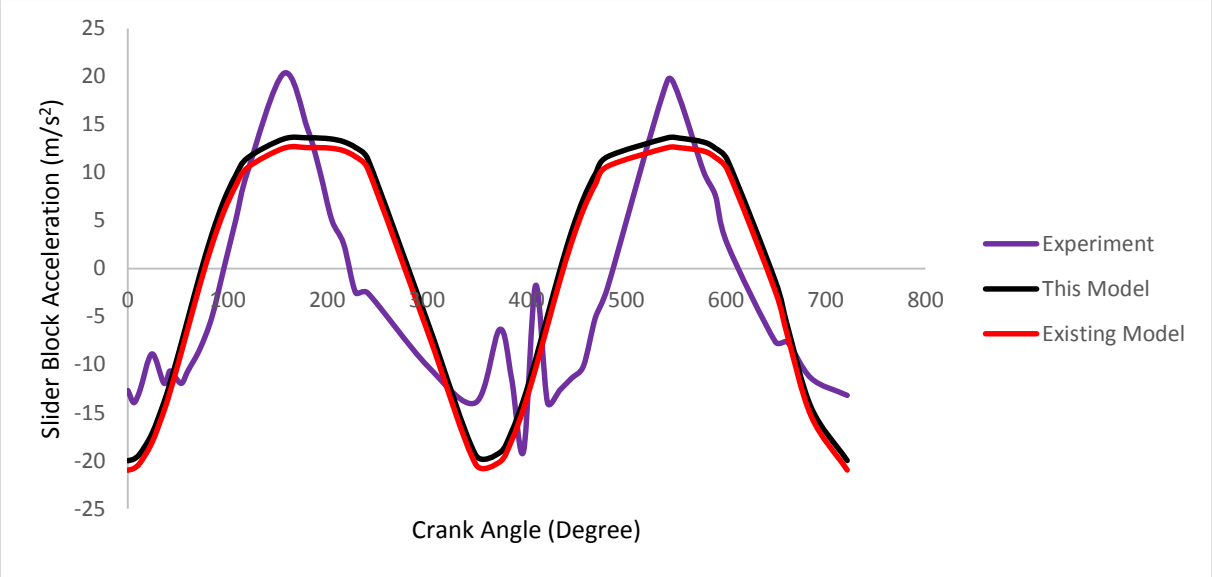

Fig. 19: Comparing torque with experimental values at e = 0mm

Table 3: Models comparison with experimental values

Data description	Experiment	This model	Existing model
Maximum Acceleration	19.56 [m/s^2]	13.58 [m/s^2]	12.59 [m/s^2]
Minimum Acceleration	-13.97 [m/s^2]	-19.98 [m/s^2]	-20.99 [m/s^2]
Maximum Error	n/a	16.24 [m/s^2]	16.30 [m/s^2]
Minimum Error	n/a	0.3678 [m/s^2]	0.3715 [m/s^2]

The results of the comparison show that the model in this study compete well with existing model, however, both models show little deviations from the experimental results. These might be as a result of some inconsistencies in the experiment due to imperfect construction, clearance distances, the featuring of the machine, unsteady angular speed, non-uniform gas pressure and errors in the measuring instrument. Nevertheless, the model developed in this work has an advantage over the existing model as it predicts torque and forces on the slider-crank mechanism at different offset positions.

5. Conclusions

Slider-crank mechanism modeling is necessary to ensure accurate design and development of such mechanism. To ensure this happens, models need to be as accurate as possible. In this work, crank slider mechanism has been modeled using both geometry and trigonometry. The equations were developed without using "approximate identities". The resultant kinematic and dynamic models were tested and analyzed. The results were found to be better and compete favorably with existing models on crank slider mechanism. The model proposed in this work can be used to predict the maximum torque a mechanism can produce when in an offset position. The effect of offset distance on torque can be studied using this model. This means that systems that needs such high torque can be properly designed using this model. Systems such as reciprocating pumps, compressors and feeders which need higher torques in their advance stroke can be appropriately designed.

Conflicts of interest

The authors said to the best of their knowledge there was no conflict of interest at the time of this study.

Funding

No fund received; it was self-sponsored.

References

Bhupesh, C. and Man, M.S. (2013) Design and Optimization of Slider and Crank Mechanism with Multibody Systems. International Journal of Science and Research (IJSR) ISSN (Online): 2319-7064.

Boyle, W.P. and Liu, K. (1997) The Offset Slider Crank: Kinematic Pseudographic Analysis. Int. J. Engng Ed. 13(3):198-203.

Doyoung, C., Jeongryul, K., Dongkyu, C., Kyu-Jin, C., TaeWon, S. and Jongwon, K. (2013) Design of a slider-crank leg mechanism for mobile hopping robotic platforms. Journal of

Mechanical Science and Technology, 27(1):207-214.

Eric, B., Chris, D. and Zachary, K. (2013) Slider-Crank Mechanism for Demonstration and Experimentation (MQP). Worcester Polytechnic Institute (WPI), 100 Institute Road Worcester, MA01609-2280.

Gulsuner, S., Walsh, T., Watts, A.C., Lee, M.K., Thoraton, A.M., Casadei, S., Rippey, C. and Shahin, H. (2013) Spatial and Tenporal Mapping of De-Novo Mutations in Schizophrenia to a Fetal Prefrintal Cortical Network.Cellpress, 154(1):518-529.

Gregory, B.D. and Katia, L.C. (2011) Analysis of the dynamics of a slider–crank mechanism with hydrodynamic lubrication in the connecting rod–slider joint clearance. Mechanism and Machine Theory, 46(2011): 1434-1452.

Hailemariam, N. (2015) Kinematics and Load Formulation of Engine Crank Mechanism. Mechanics, Materials Science. Engineering Journal.

Hroncová, D., Frankovský, P. and Bettes, G. (2016) Kinematical Analysis of Crank Slider Mechanism with Graphical Method and by Computer Simulation. American Journal of Mechanical Engineering, 2016, 4(7):329-343.

Jomartov, A. A., Joldasbekov, S. U., and Drakunov, Y. M. (2015) Dynamic synthesis of machine with slider-crank mechanism. Mech. Sci., 6: 35–40.

Kittur, R.A. (2017) Design and Force Analysis of Slider-crank mechanism for Film Transport Used in VFFS Machine. International Research Journal of Engineering and Technology (IRJET) e-ISSN: 2395-0056 4(12): 25-35.

Mohammad, R., Mansour, R., Abdol, H.H., Kamran, K. and Mohammad, R.A. (2011) Kinematics and kinetic analysis of the slider-crank mechanism in otto linear four cylinder Z24 engine. Journal of Mechanical Engineering Research, 3(3):85-95.

Patel, S.R., Patel, D.S. and Patel, B.D. (2013) A Review on Kinematic and Dynamic Analysis of Mechanism. International Journal of Engineering Science and Innovative Technology (IJESIT), 2(2): 338 -341.

Peter, F. and Darina, H. (2015) Kinematic analysis of the crank mechanism with rotating cylinder using MSC Adams/View. Applied Mechanics and Materials Submitted: 2015-04-28. ISSN: 1662-7482, 8(16): 213-223.

Rudolf, T., Momir, S. and Zoran, L. (2012) The Optimization of Crankshaft Offset of Spark Ignition Engine. Journal of Trends in the Development of Machinery and Associated Technology, 16(1):211-214.

Sahidur, R. (1991) Dynamic Analysis of the Generalized Slider Crank. A Thesis Submitted to the Faculty of the Graduate Division of the New Jersey Institute of Technology in Partial Fulfillment of the Requirements for the Degree of Master of Science Department of Mechanical Engineering.

Santosh, M., Vishal, F., Vedali, C.,Yashaswini, D. and Rohit, N. (2018) Slider-crankMechanism. International Journal of Advance Research in Science and Engineering, 7(3): 5-15.

Sarigeçili, M.I. and Akçali, I.D. (2018) Dynamic Modeling of Slider-Crank Mechanism for Selecting Input Parameters for Desired Piston Speeds: Lumped Mass Approach. Çukurova University Journal of the Faculty of Engineering and Architecture, 33(4): 67-82.

Thaddaeus, J. (2016) Synthesis and Dynamic Simulation of an Offset Slider-Crank Mechanism. International Journal of Scientific and Engineering Research, 7(10):1842 ISSN 2229-5518.